The Peculiarities of Tungsten's Influence on Phase Transformations and Mechanical Properties of the Directionally Solidified HCR Nickel-Base Alloy

V.V. Ivanov and W.G. Ferguson

The University of Auckland, New Zealand
Department of Chemical and Materials Engineering

(Received September 1,1999.)

ABSTRACT

The application of the directional solidification (DS) increases the life of turbine blades. But this technology demands a new alloying approach, especially for the nickel-base, hot corrosion resistant (HCR) alloys. Such an approach was undertaken in this investigation. The influence of tungsten on the microstructure, phase content, phase transformations, and mechanical properties of the HCR nickel-base alloys were studied both in equiaxially and directionally solidified conditions. Tungsten content was varied between 3 to 9%. Samples with equiaxially and directionally solidified structures were obtained in a High Gradient Directional Solidification Unit with the liquid metal coolant (LMC). The LMC was molten aluminium. It was shown that tungsten has the effect of strengthening the dendrites, which further promotes the DS. The maximum mechanical properties of the directionally solidified alloy were obtained at tungsten content of 7% versus 5% for the conventionally solidified alloy.

INTRODUCTION

In order to increase the life of turbine blades the main areas of weakness must be eliminated, i.e. transverse grain boundaries. The application of directional solidification is a method of achieving this. In general alloys have different abilities to directionally solidify /1/, depending on the amount of secondary phase and their precipitating temperatures, the elements that strengthen the grain boundaries, and other features. The inherent features of the aircraft nickel superalloys (low chromium content, high tungsten and aluminium content) predetermine good directional solidification behaviour for these alloys. In marine and industrial gas turbines alloys with hot corrosion resistance (HCR) are used. But conventional nickel HCR alloys because of their alloying features (high chromium content, relatively low tungsten and aluminium content) have inferior directional solidification behaviour compared to aircraft alloys. The gain in creep resistance from applying directional solidification to HCR alloys is only about 20-30% /2/. Thus there is a need for developing the nickel HCR alloys for directional solidification.

The nickel-base superalloys are optimally alloyed materials and simple adding of more elements leads to overalloying and drastically reduces the service properties of the alloy. Thus, investigation of the alloying mechanism of the HCR nickel-base superalloys for directional solidification is required.

There are several methods of directional solidification. They differ in the way in which the temperature gradient is created. The most popular method of manufacturing turbine blades is the so-called "HRS-process" in which the mould with molten alloy moves out from the heated zone at a controlled rate and the columnar grains grow from the cooling bottom of the mould to the top.

The essential disadvantage of this method is the increasing distance between the cooling surface and the crystallization front during the solidification process. As a result, the temperature gradient decreases giving

coarse-structural constituents at the upper part of the casting. Increasing of dendrite arm spacing leads to transition from single-crystal solidification to equiaxed solidification. Pollock and Murphy /3/ reported that when the thermal gradient was decreased to levels below 15 °C/cm complete breakdown of single-crystal solidification by equiaxed grains of nickel-base superalloys occurred.

Further improvement of the heat transfer conditions and an increase of the temperature gradient are possible by using a liquid metal coolant (LMC) with melting point lower than the alloy melting point. As the mould submerges into the bath with liquid metal coolant, directional solidification occurs. This method, the cold "HGS-process" or "LMC-process", has several advantages in comparison with the "HRS-process", such as /4, 5, and 6/:

- permits positioning of the crystallization front relative to the coolant level, allowing a uniform columnar structure to form in complicated geometrical forms and long components;
- permits an increase in the solidification rate by between 2-3 times, that significantly reduces the size of all micro-structural constituents;
- permits an independent control of the temperature gradient and crystallization rate that is impossible in other methods.

In this investigation samples with a directionally solidified structure were obtained by using the LMC-process.

PROCEDURE

Materials

A common industrial HCR nickel-base alloy with composition, % (weight): C – 0.09; Cr – 15.8; Co – 11.0; W – 5.5; Mo – 2.0; Al – 2.8; Ti – 4.5; Nb – 0.3; Zr – 0.05; Y – 0.005, was chosen as the base alloy for the investigation. The main properties of this alloy at 900°C are: ultimate tensile stress - 727 MPa; 100 hour rupture stress - 250 MPa; creep rupture elongation - 6-8%; creep rupture reduction of area - 10-20%.

The influence of tungsten content, which varied between 3-9%, on alloy microstructure, phase transformations and mechanical properties was studied for both equiaxially and directionally solidified conditions.

The equiaxially and directionally solidified structures were produced in a High Gradient Directional Solidification Unit with a liquid metal coolant. The liquid metal coolant was molten aluminium. A schematic diagram of this unit is shown in Figure 1.
The parameters of the directional solidification process were:

- the temperature of the mould heating furnace 1600°C;
- the temperature of the second zone heater 1550°C;
- the temperature of the LMC 880 ± 20°C;
- the velocity of the mould movement 17×10^{-5} m/s.

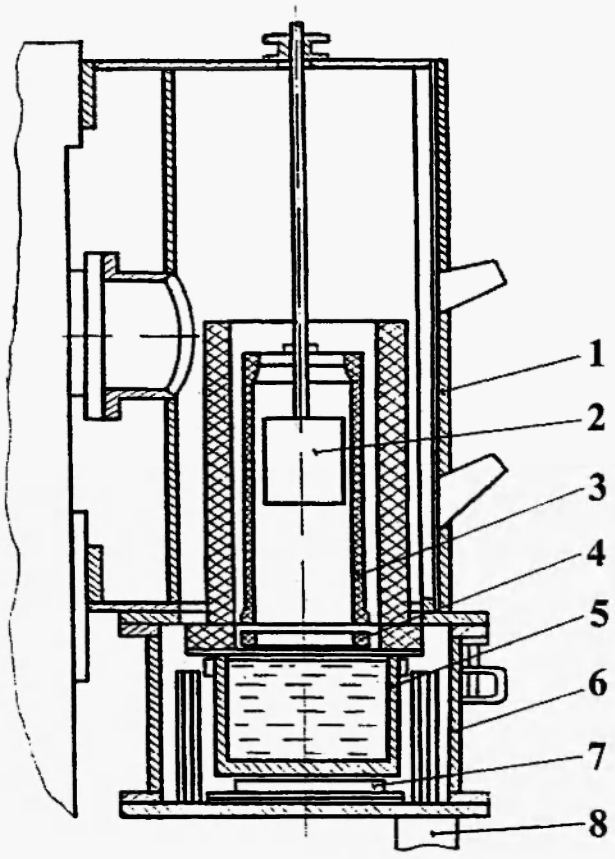

Fig. 1: A schematic drawing of the high gradient DS unit. 1 – upper chamber; 2 – ceramic mould; 3 – mould-heating furnace; 4 – second zone heater; 5 – bath with liquid metal coolant; 6 – bottom chamber; 7 – bottom heater; 8 – lifting mechanism.

Microstructural Analysis.

The etch used to reveal the general microstructure of the polished samples was Vasiliev's reagent: 500 ml of hydrochloric acid, 25 ml of sulfuric acid, and 100 g of copper sulfate.

Phase Analysis.

The phase structure and composition were studied using a physico-chemical method, which included electro-chemical separation of the phases followed by XRD and chemical analysis of the isolated phases.

The γ′- phase and carbides were extracted with a general electrolyte (10 g of the citric acid, 10 g of the ammonium sulfate, and 1200 ml of water) with a residence time of 45-60 min and a current density of 500-600 a/m^2. The γ - solid solution dissolves, but the γ′-phase and carbides remain on the anodic sample (anodic sediments).

The XRD analysis of the monoliths and anodic sediments was done with an X-ray diffractometer, DRON-3, using monochromatic $Cu_{K\alpha}$ radiation (7).

SEM and EDX Analysis.

Microsegregation of the alloying elements in alloys with different structure types was examined with a "JCXA-733" X-ray microanalyser. The morphology, size and distribution of the γ′- phase were studied on the same equipment in the SEM mode.

Differential Thermal Analysis (DTA).

The temperatures of the main phase transformations for each alloy studied were determined with a VDTA-8M3 device using the DTA method (8).

The standard sample was a tungsten monocrystal. The specimens were heated and cooled at a rate of 0.6°C per second in an argon atmosphere at pressure 5.0 × 10^4 Pa.

Mechanical Testing.

The ultimate tensile stress, elongation and reduction of area of the alloys at high (900°C) and ambient temperatures were determined according to standard: GOST 1497-84. Cylindrical samples with initial diameter d_0 = 5 mm and initial length $l_0 = 5\ d_0$ were used.

The 100 hour rupture stress, creep rupture elongation and reduction of area of the alloys at 900°C were determined according to standard: GOST 10145-81. Cylindrical samples with initial diameter d_0 = 5 mm and initial length $l_0 = 5\ d_0$ were used.

RESULTS AND DISCUSSION

Tungsten mostly dissolves in the nickel superalloy matrix where it is known to be an effective solid solution strengthener /9,10/. It can be seen from the chemical analysis results (Table 1) that tungsten also dissolves in the intermetallic γ′- phase and carbo-boride phases. Whereas the tungsten concentration in the γ′-phase increases slightly, the amount of the strengthening phase remains essentially constant. As the tungsten concentration increases from 3.0% to 9.0%, the carbo-boride phases weight fraction increases from 0.82% to 1.17%. Thus, the chemical analysis would indicate that the increased amount of tungsten in the nickel-base superalloys goes primarily into alloy solid solution and carbo-boride phases, increasing the amount of carbo-boride phases, with very little increased tungsten content in the γ′- phase.

The XRD results indicate that the carbide phase changes from TiC at W 3.0% and 5.0% to (Ti,W)C at W 7.0% and (Ti,Cr,W)C at W 9.0% (Table 2). Tungsten substitutes for the titanium atoms in TiC, decreasing the carbide lattice parameter from 4.341 Å at W 3.0% to 4.328 Å at W 9.0%. The excess titanium goes to creating titanium boride TiB_2, and η- phase Ni_3Ti, but the presence of the last was not confirmed. A small amount of molybdenum di-boride MoB_2 and carbide $(Mo,Cr,Co,Ni)_6C$ were found in the testing alloys.

With increasing tungsten content the lattice parameter of γ -solid solution increases from 3.575 Å to 3.593 Å, whereas the lattice parameter of the γ′- phase is essentially constant, and the mis-fit strain parameter $\Delta a_{\gamma\text{-}\gamma'} = [(a_\gamma - a_{\gamma'}) / a_\gamma] \times 100\%$ decreases from –0.448 to 0.0% (Table 2).

From a thermodynamic point of view the maximum stability will be achieved in an alloy with a minimum

Table 1

The Influence of Tungsten on the Chemical Composition And Quantity of Strengthening Phases

W % (wt)	Elements content in alloy, % (wt)							The amount of carbide phase % (wt)
	Ni	C	Cr	Co	Al	Ti	Mo	
3.05	60.47	0.10	15.01	11.46	3.43	4.70	1.78	0.82
5.02	58.48	0.10	15.51	10.96	3.32	4.80	1.81	0.94
7.11	56.67	0.11	15.30	10.80	3.28	4.81	1.92	1.05
8.93	54.41	0.12	15.47	11.10	3.33	4.78	1.86	1.17

W % (wt)	Elements content in γ'- phase, % (wt)							The amount of γ'- phase % (wt)
	Ni	Cr	Co	Al	Ti	Mo	W	
3.05	76.08	1.88	6.70	4.63	9.01	0.51	1.19	41.06
5.02	76.03	1.89	6.74	4.61	9.06	0.51	1.17	41.63
7.11	76.04	1.86	6.71	4.62	9.01	0.48	1.28	41.30
8.93	75.90	1.89	6.69	4.61	9.02	0.49	1.40	40.80

Table 2

Alloy Phase Compositions with Different Tungsten Content

W % (wt)	Identified phases		The lattice parameter Å	$\Delta a_{\gamma-\gamma'}$ %
	Main peaks	Weak peaks		
3.0	γ-solid solution γ'-phase Ni_3Ti TiC	MoB_2	3.575 3.595 4.341	-0.448
5.0	γ-solid solution γ'-phase Ni_3Ti TiC	MoB_2	3.581 3.592 4.337	-0.307
7.0	γ-solid solution γ'-phase Ni_3Ti (Ti,W)C	$(Mo,Cr,Co,Ni)_6C$; MoB_2 TiB_2	3.587 3.592 4.332	-0.139
9.0	γ-solid solution γ'-phase Ni_3Ti (Ti,W)C	η-phase Ni_3Ti $(Mo,Cr,Co,Ni)_6C$; MoB_2 TiB_2	3.593 3.593 4.382	0.0

surface energy on the interface between γ - and γ′-phases, i.e. with minimum $\Delta a_{\gamma-\gamma'}$ (9). Thus, the maximum thermostability of the alloys studied will be at W 9.0%.

In connection with this it is necessary to mention another important feature of the mis-fit strain parameter. It was noted that a columnar structure was more readily obtained in the alloys with minimum $\Delta a_{\gamma-\gamma'}$. It has been reported for directionally solidified alloys that when processing conditions and other parameters are equal, alloys with a minimum $\Delta a_{\gamma-\gamma'}$ have less macrostructural defects (large-angle boundaries, triple points, and so on). This, apparently, results from the amount of lattice defects in the matrix, which eventually accumulate on the phase interfaces. The presence of such defects leads to the breakdown of the regular structure and to the nucleation and growth of disorientated dendrites. As the $\Delta a_{\gamma-\gamma'}$ reduces, the interface surface energy decreases and thus the number of lattice defects on the interface decreases. This is most likely to occur in those alloys where decomposition of the supersaturated solid solution and precipitation of the strengthening γ′- phase starts during the solidification process. The mis-fit strain parameter becomes very important in manufacturing single crystal blades, where the amount of mis-orientations should be kept to an absolute minimum.

Thus, the HCR alloys represent a heterogeneous system, the main contributors of which are: γ - solid solution, intermetallic γ`- phase, carbides, borides, eutectic γ / γ′, and sometimes, η - phase of a type Ni_3Ti. Transformations of structural and phase conditions occur during heating of these alloys. Such processes, like destruction of a short-range order; dissolution of γ′-phase, carbides and borides; melting of eutectic phases and γ - solid solution take place in these alloys. All these processes occur in backward order during a cooling. The main transformations in alloys during heating/cooling and their temperature ranges, depending on alloy content were identified using differential thermal analysis (DTA) (Figure 2). A significant feature of the DTA curve is the melting peak, which is the highest. The melting temperature range is given by the right-hand side: the onset of melting is given by the first decrease from the peak and the end of the melt – by the minimum of the curve /8/.

The differential thermal analysis results (Figure 2)

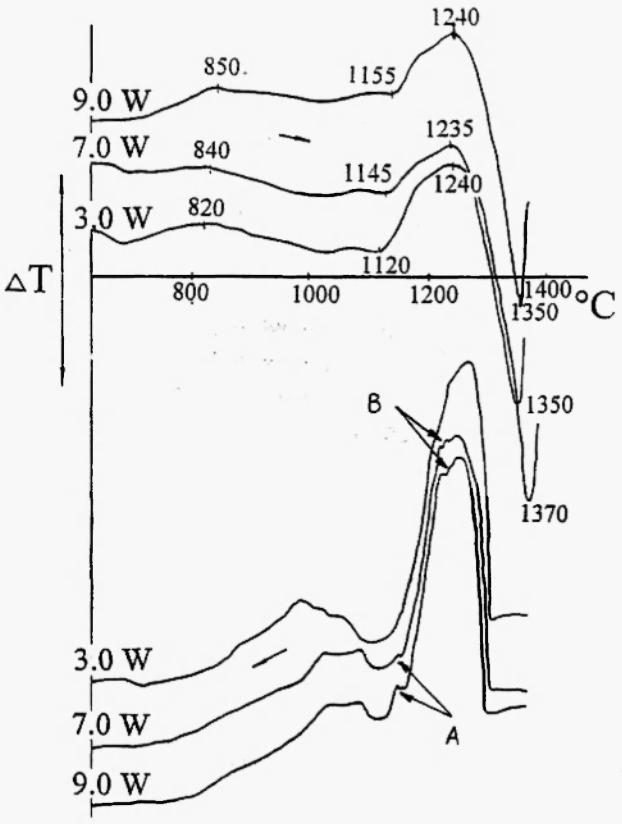

Fig. 2: The dependence of DTA curves on tungsten content.

show that increasing tungsten content has a little effect on the solidus, being in the range 1235 - 1240°C, but decreases the liquidus from 1370°C to 1350°C. Thus the crystallization interval $\Delta T = T_L - T_S$ of the alloy is reduced from 130°C to 110°C. The reduction of ΔT reduces the mushy zone ahead of the liquid/solid interface and, as a consequence, casting segregation.

The exothermal peaks on the falling branches of cooling curves (Figure 2, arrows A) relate to the formation of eutectic γ / γ′ (8). It can be seen from the figure that the alloy with 9.0% W contains more eutectic structure than the alloy with 7.0% W.

Clearly marked peaks for carbide dissolution are not observed on the heating curves (Figure 2, top curves). This is because of the small amount of carbide present (~1.3%). Even so, the "B" indications on the cooling curves near the top of crystallization peaks for 7.0% W and 9.0% W alloys may reflect the following carbide transformation:

$$MC + \gamma = M_6C + \gamma'$$

This presumption correlates with the results of phase analysis (Table 2).

The temperature interval over which the γ'- phase dissolves precedes the melting temperature. It is very difficult to determine the temperature at which the γ'-phase dissolution commences, because in the same temperature range other transformations (like destruction of short-range order and coagulation of the γ`-phase) occur. Also, the dissolution of the γ'- phase is complicated, because the composition and morphology of the intermetallic compounds in the dendritic and interdendritic locations differ. It can be seen that tungsten shifts the peaks of the γ'- phase transformations into a region of higher temperatures. As indicated in Figure 2, tungsten shifts peaks from 820°C to 850°C and from 1120°C to 1155°C in the middle and upper end of the dissolution temperature range. This indicates that tungsten increases the thermostability of the γ'-phase in these alloys.

Dendritic cells represent the microstructure of the directionally solidified alloys (Figure 3). Particles of primary carbo-borides and intermetallic phases are observed in interdendritic position. With increasing tungsten content the number and sizes of these particles increases, resulting in blocking dendritic growth and reducing dendritic size.

The microstructure in the equiaxially solidified alloys in the near-boundary regions changes with increasing tungsten content (Figure 4), from finely divided carbo-boride particles at low tungsten content to coarse particles with adverse shape at higher tungsten concentrations. Also, colonies of eutectic γ/γ' are observed in the microstructure of the alloy with 9.0% W.

Such microstructural transformations are accompanied by changing mechanical properties (Figures 5 and 6). The results of tensile tests and 100-hour rupture stress tests at 900°C are shown in Figures 5 and 6. Tungsten increases the short-time creep (ultimate) strength in the alloy range investigated, reaching a maximum at 7.0 – 9.0% W (Figure 5). In contrast, for the long-time creep strength (Figure 6) the equiaxially solidified structure is preferable for such loading conditions. This confirms that different loading conditions have different fracture mechanisms. With short-time creep tests (maximum stresses, short-time acting, high temperature) both transgranular and

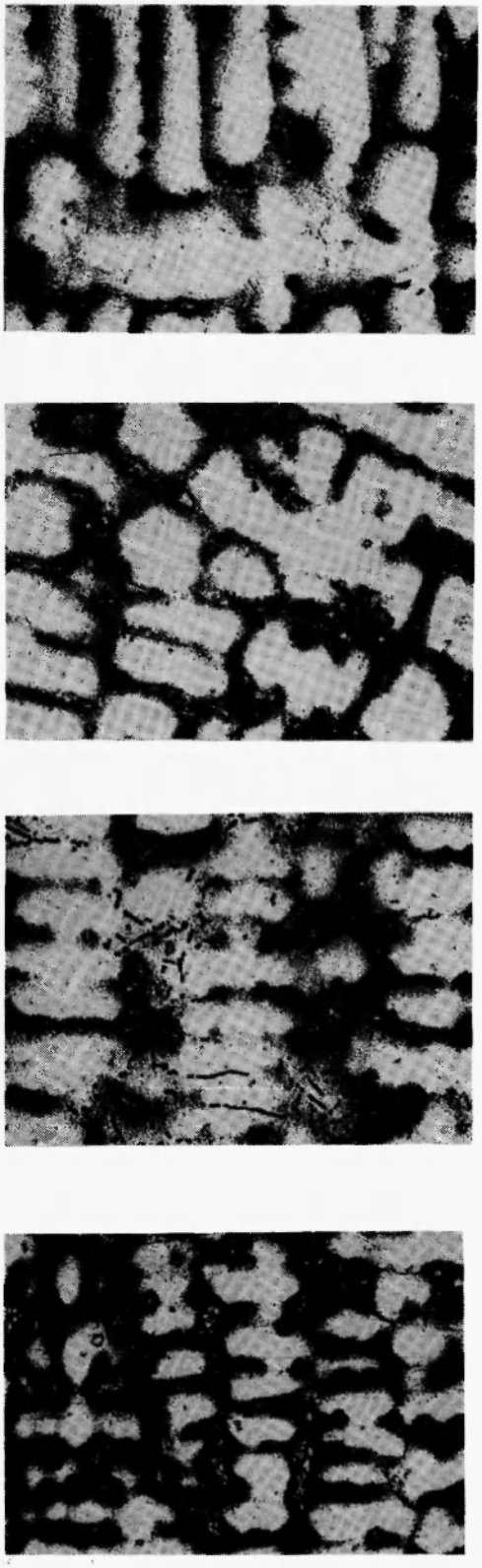

Fig. 3: Directionally solidified alloy microstructure dependence on tungsten content, 300 ×.

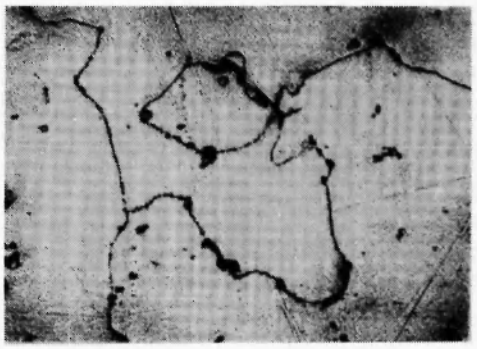

3.0%

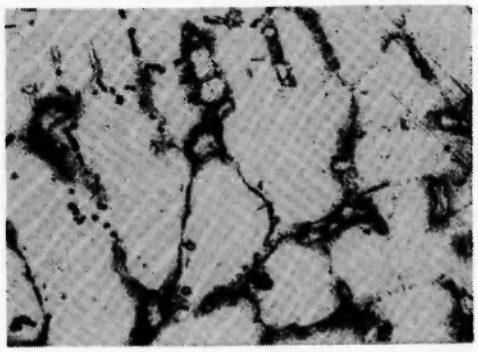

5.0%

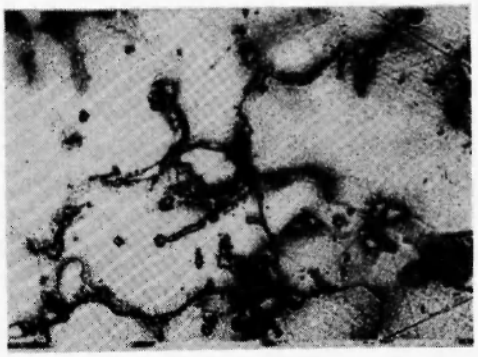

7.0%

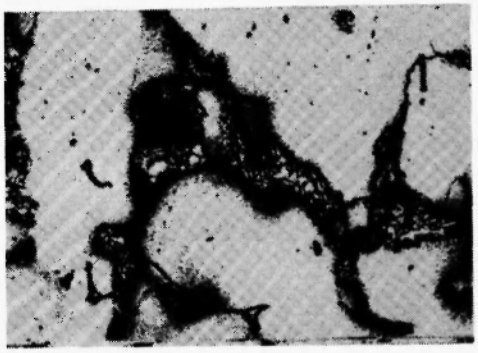

9.0%

Fig. 4: Equiaxially solidified alloy microstructure dependence on tungsten content, 300 ×.

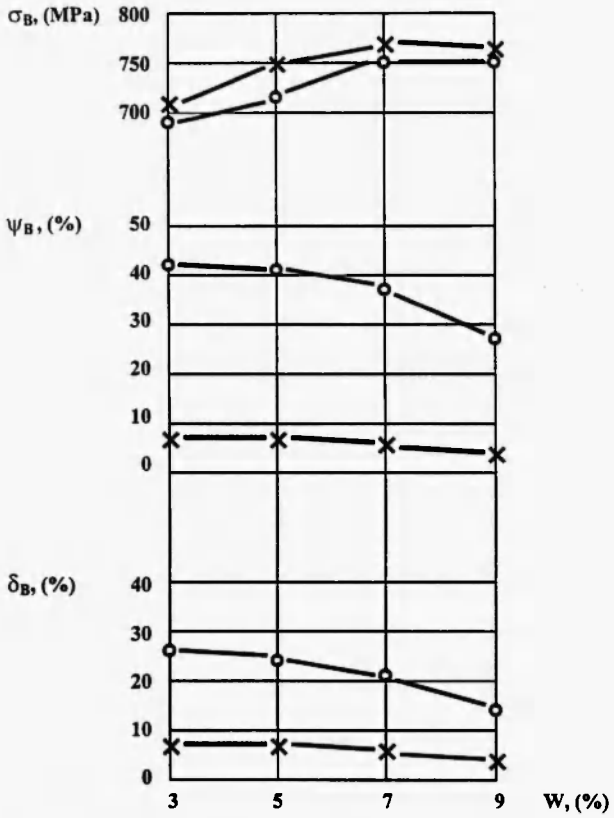

Fig. 5: Mechanical properties [ultimate strength (σ_B), reduction of area (ψ_B), elongation (δ_B)] of the equiaxially (×) and directionally (o) solidified alloys at 900°C versus tungsten content.

intergranular fracture occur. Under such loading conditions plastic deformation occurs as a result of dislocation motion along the most close-packed planes and grain boundary sliding. The grain boundary precipitates impede boundary migration and, consequently, the more carbo-boride and intermetallic phases that precipitate at grain boundaries the higher the ultimate strength of material.

In a high temperature long-time test the grain boundaries are the most favourable places for microvoid nucleation and growth /10/. These microvoids are formed from grain boundary precipitates and vacancy condensation. In this case fracture occurs along the grain boundaries, normal to the direction of maximum tensile stress. More over, the high density of dislocations near the grain boundaries leads to a loss of the coherent bands between the lattices of γ- and γ′-

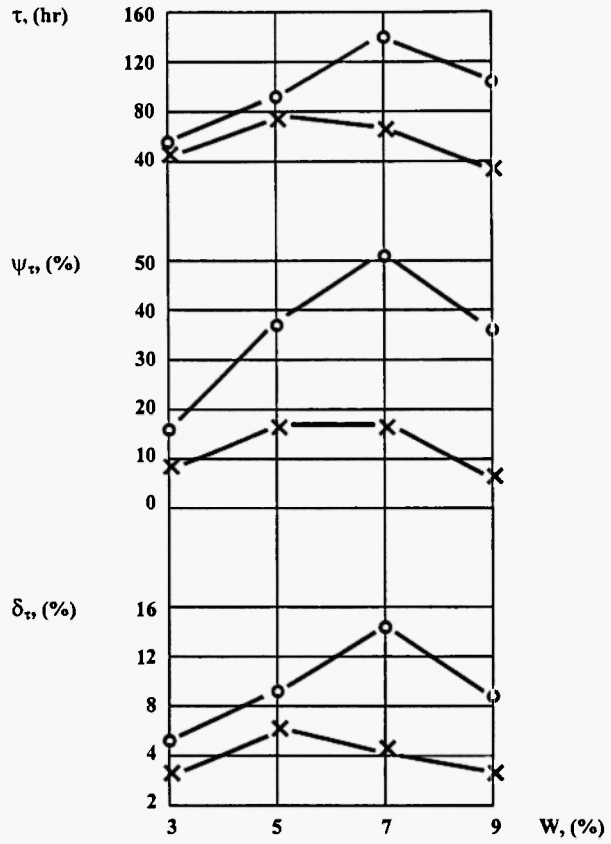

Fig. 6: Creep rupture properties [time to fracture (τ), reduction of area (ψ_τ), elongation (δ_τ)] of the equiaxially (×) and directionally (o) solidified alloys at 900°C and load 300 MPa versus tungsten content.

phases. Thus, alloys with conventionally solidified equiaxed grains have inferior performance in creep to materials with directionally solidified structures.

Reduction of area ψ_B and elongation δ_B in the short-time test decreases with increasing tungsten concentration independently of the type of structure (Figure 5). However, the ductility values of directionally solidified alloys are significantly higher than for equiaxially solidified alloys. This can be explained by the small size of precipitates, their uniform distribution, less microporosity and less microsegregation for directional solidification /11/.

For long-time creep tests, time to fracture, τ, at 900°C and under a constant stress of 300 MPa, creep rupture elongation, δ_τ, and reduction of area, ψ_τ, versus tungsten concentration show a maximum (Figure 6). The interpretation of these curves is of interest for making clear the alloying features necessary for directional solidification. When the tungsten concentration is increased to 5% the creep rupture time increases for both the equiaxially and directionally solidified structures, with the latter giving only about 25% improvement in performance. Increasing the tungsten content to 7.0% leads to a significant differentiation in behaviour.

Firstly, this can be explained by tungsten segregation, which concentrates to a greater degree in the dendrites (Figure 7). This means that tungsten mostly strengthens the dendrites rather than interdendritic space, where grain boundaries are situated. Molybdenum, also a matrix strengthener, unlike tungsten does not have such a strong tendency to dendrite segregation (Figure 8); rather it is more uniformly spread through the dendritic and interdendritic spaces. As there is molybdenum in the interdendritic space it gives more enhancement of grain boundary strength. Thus to achieve the maximum strengthening in nickel-based conventional superalloys it is necessary to have both elements present, with tungsten enhancing the dendrites and molybdenum enhancing the interdendritic space and grain boundaries. During directional solidification, grain growth is in the longitudinal direction, total grain boundary area is decreased and there are no transverse boundaries. Thus the elements which improve the creep strength of the grains become more important than the elements which increase grain boundary strength. Since the tungsten content in the nickel HCR alloys is low (~ 5%), its contribution to dendrite strengthening is not high. For this reason the improvement in performance by directional solidification is only about 25-30% (see above). From Figure 6 it can be seen that by increasing of tungsten content there is marked improvement in performance of the nickel HRC alloys by directional solidification.

Secondly, the maximum mechanical properties for directionally solidified alloys are achieved at higher tungsten content than for conventionally solidified ones because there is less chemical heterogeneity with directional solidification and this allows more alloying elements to dissolve without overalloying (Figure 8). This is possible because the solid/liquid zone ahead of

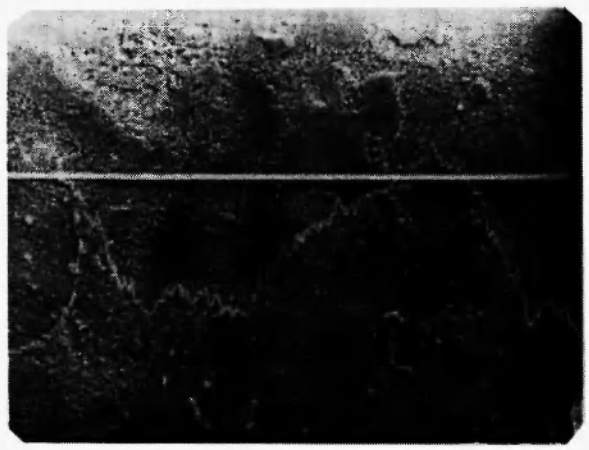

a

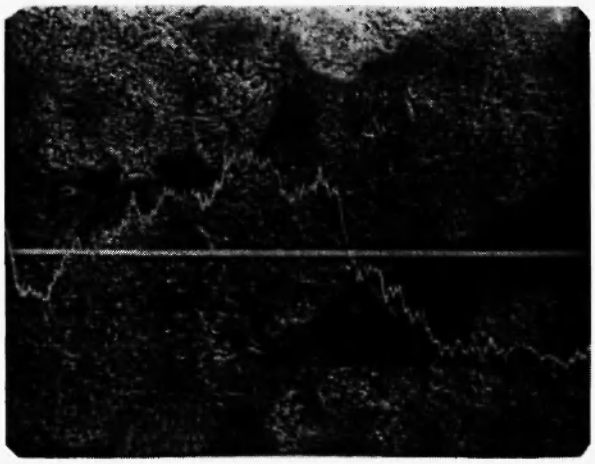

b

Fig. 7: Tungsten microsegregation in equiaxially (a) and directionally (b) solidified alloys, 1000 ×.

a

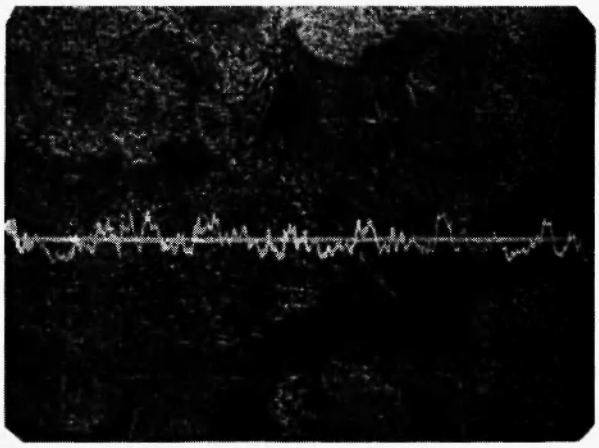

b

Fig. 8: Molybdenum microsegregation in equiaxially (a) and directionally (b) solidified alloys, 1000 ×.

the growth interface is small and constant during directional solidification. This is a particular feature of the LMC-process compared with other directional solidification techniques /5/.

Thus, the maximum mechanical performance of nickel-base HCR alloys for directional solidification is achieved at tungsten content between 6.5 – 8.0%.

CONCLUSIONS

1. Raising tungsten content from 3% to 9% increases the dissolution temperature of the γ′- phase by 35°C, thus improving the thermostability of the alloys studied.
2. Tungsten decreases the mis-fit parameter of the

matrix lattice and strengthening phase lattice, $\Delta a_{\gamma-\gamma'}$, lessens the interphase energy on the γ/γ' interface and thus reduces the amount of defects and makes it easier to get a regular oriented structure.

3. Tungsten increases the quantity and changes the composition of the carbides, thus promoting the alloy strength.
4. Tungsten decreases the crystallization interval of the alloys studied by 20°C. This in combination with the LMC-process allows reduction of the solid/liquid zone and, as a consequence, a reduction of casting segregation.
5. The maximum mechanical properties of the directionally solidified alloy were attained at tungsten content of 7% and at 5% for the equiaxially solidified alloy. Tungsten has the effect of strengthening the dendrites, which further promotes directional solidification.
6. The optimum tungsten concentration in HCR alloys for directional solidification is between 6.5 – 8.

REFERENCES

1. K. Saiga, "Modern superalloys"; *Kikay No Kanku;* **1**, 191-196 (1977).
2. V.V. Ivanov, E.N. Fedotov, G.F. Mylnitsa *et al*; "The Influence of the Directional Solidification on the Properties of the Nickel Alloy"; NSI Transactions; Nikolaev: Nikolaev Shipbuilding Institute, 1983.
3. T.M. Pollock and W.H. Murphy. "The breakdown of single-crystal solidification in high refractory nickel-base Alloys"; *Metallurgical and Materials Transactions A*, **27 A**, 1081 – 1094 (1996).
4. V.V. Ivanov, E.N. Fedotov and V.B. Timofeev, "To the question of the high-rate directional solidification of the heat-resistant and corrosion resistant alloys"; Thesis of the All-Union Scientific and Engineering Conference "Physicochemical Aspects of the Heat Resistant Inorganic Materials Strength", Zaporogye, 1986; p.45.
5. J.S. Erickson; "Modern processing methods and investment casting of the superalloy family"; *High-Temperature Materials Gas Turbine;* Amsterdam, 1974; pp.315-340.
6. Y.I. Zvezdin, E.L. Kats, Y.V. Kotov, et al. "New corrosion-resistant nickel-base superalloys and technological processes of casting gas turbine parts with directional single crystal and regulable equiaxial minimized microporosity structure"; *Conference: Mechanical Behaviour of Materials:* VI, Vol.2, Kyoto, Japan, 29 July – 2 Aug, 1991, Pergamon Press p/c (UK), pp. 111 – 116, 1992.
7. Y.S. Usmanskiy, U.A. Skakov, A.N. Ivanov et al; "*Crystallography, Roentgenography and Electron Microscopy*"; Moscow, Metallurgiya, 1982; 632 p.
8. V.A. Vertogradskiy and T.P. Rykova, "Studying of the phases transformations in the type GS alloys by the DTA method"; *The Heat Resistant and Heat Durable Steels and Alloys on the Nickel Base;* Moscow; Nauka, 1984; pp23-227.
9. C.T. Sims and V.C. Hagel, "*Heat Resistant Alloys*"; Moscow, Metallurgiya, 1976; 568p.
10. I.A. Oding, V.S. Ivanova and V.V. Burdunskiy, "*The Theory of Creep and Endurance Strength of Metals*"; Moscow; Metallurgisdat, 1958; 488p.
11. M. Flemings, "*Solidification Processes*"; Moscow; Mir, 1977; 423p.